Desalination and Water Treatment
www.deswater.com

doi:10.5004/dwt.2018.22695

124 (2018) 106–116
August

Effective removal of heavy metals from aqueous solution by porous activated carbon/thiol functionalized graphene oxide composite

Fatemeh Mojoudi[a], Amir Hossein Hamidian[a,*], Nooredin Goodarzian[b], Soheil Eagderi[c]

[a]*Department of Environment, Faculty of Natural Resources, University of Tehran, Karaj, Alborz, Iran, email: fatemehmojodi@yahoo.com (F. Mojoudi), Tel. +98-263- 222 3044, email: a.hamidian@ut.ac.ir (A.H. Hamidian)*
[b]*Department of Applied Chemistry, Shiraz Branch, Islamic Azad University, Shiraz, Fars, Iran, email: ngudarzian@yahoo.com (N. Goodarzian)*
[c]*Department of Fisheries, Faculty of Natural Resources, University of Tehran, Karaj, Alborz, Iran, email: soheil.eagderi@ut.ac.ir (S. Eagderi)*

Received 22 January 2018; Accepted 28 June 2018

ABSTRACT

As a result of need to develop effective adsorbents for water pollution treatment, in present study, a novel composites from thiolated graphene oxide (TGO) and activated carbon (AC) was prepared from sugar cane molasses using a one-step chemical activation process by KOH and $ZnCl_2$. KAC/TGO and ZAC/TGO, were successfully synthesized and characterized by Brunauer–Emmett–Teller (BET) surface area analysis, iodine adsorption, Fourier transform infrared (FTIR)spectroscopy, X-ray diffraction (XRD) and scanning electron microscopy (SEM). Among produced ACs and composites, KAC/TGO possesses higher specific surface area of 1044 m^2/g, a total pore volume of 0.998 m^3/g and iodine number of 920 mg/g. Results of heavy metals removal experiments with KAC/TGO in aqueous solution showed that the Langmuir model fitted better than Freundlich model with a maximum adsorption capacity of 204.08 and 196.07 mg/g for Pb(II) and Cu(II) respectively which is higher than many other adsorbents. Also the pseudo-second order kinetic model was found to agree well with the experimental data for both Pb(II) and Cu(II) adsorption. It is expected that this novel and low cost adsorbent can be effectively used for removal of heavy metals from the aqueous polluted environment.

Keywords: AC/TGO Composite; Characterization; Adsorption; Heavy metals; Isotherm; Kinetic

1. Introduction

Heavy metals have exponentially increased in the aquatic environments due to industrial and agricultural activities. Prolonged exposure to heavy metals can cause serious threats to human health and other biological systems, especially when the levels of heavy metals are exceeded beyond their tolerance [1]. There are several treatment techniques to remove heavy metals from the contaminated aquatic environments, including chemical precipitation, oxidation or reduction, coagulation, flocculation, electro-dialysis, electro-flotation and electro-oxidation, ultrafiltration, nano-filtration, ion-exchange, reverse osmosis, disinfection, sedimentation and adsorption [2]. According to price/performance criteria, adsorption is an effective, safe, favorable, easy to operate and economical method to remove toxic metal ions from polluted waters. For this purpose, different type of materials can be applied as heavy metals adsorbents e.g. activated carbons [3], natural clays [4], zeolites [5], silicagel [6], chitosan [7], and graphene oxide [8] and composites with these materials [9–11].

Activated carbon-based composites with the other carbon allotropes are among preferred and exciting adsorbents for removal of pollutants from aqueous solutions because

*Corresponding author.

of their unique properties such as high adsorption capacity to eliminate a wide variety of toxic pollutants and low cost, especially when prepared from waste materials [12,13]. Activated carbon (AC) is prepared by carbonization of carbonaceous source materials that commonly used in a variety of applications due to possessing a relatively high porosity and large surface area. The adsorption capacity of AC is related to the chemical functional groups on the pore surfaces, internal surface area, pore size distribution and pore volume and structure [14]. Recently, more attention has been paid to increase the adsorption capacity of ACs by composition with suitable nanomaterials [13,15]. Over the last half-decade, graphene and its derivatives are among the most reliable and reproducible precursors to employ in a diverse array of uses. Preparation the composites with these nanoscale allotropes of carbon have attracted a great interest for industrial applications, since graphene was first reported in 2004 [16]. Graphene oxide (GO) is among the most promising, new research material for fabrication of an effective adsorbent due to its two-dimensional (2D) layer of sp2-hybridized carbon, high surface area, large pore volume and presence of surface functional groups such as epoxy (–COC), hydroxyl (–OH), carbonyl (–CO), and carboxyl (–COOH) groups [8]. These oxygenated functional groups improve adsorption performances and result in easy dispersability of GO in different matrixes such as water.

In the present work, we prepared the AC/TGO composite using the solution mixing method. It is interesting to investigate the adsorption properties of AC/TGO knowing the fact that GO and AC have large surface area and high adsorption capacity which play an important role in increasing its adsorption capacity. Hence, the main aim of the present study was to evaluate the ability of AC/TGO to adsorb heavy metals (lead and copper) from aqueous solution using batch adsorption technique. The results of this study can lead to inaugurate of a novel promising adsorbent with high capacity and low cost to eliminate high levels of heavy metals pollution in aquatic environments.

2. Material and methods

2.1. Materials

For the production of ACs, sugar cane molasses was obtained from the Haft Tapeh sugar cane company (Khuzestan Province, Iran) and KOH and $ZnCl_2$ from Merk Co., Inc. Also for the synthesis of GO, chemicals were purchased from Merk Co., Inc. The chemicals used for preparation of stock solutions for adsorption ($PbNO_3$ and $CuNO_3$) were obtained from Sigma-Aldrich.

2.2. AC synthesis

Two different type of ACs were made by activation of sugarcane molasses powder with a single stage activation process using KOH and $ZnCl_2$ as activating agents. The precursor was separately soaked inactivating agents in a ratio of 1:3 (by weight) for 24 h to prepare KAC and ZAC, respectively. The mixture was dried overnight at 110°C, crushed and sieved using a 30 mesh sieve. Then, the samples were placed in a muffle furnace and pyrolyzed using a heating rate of 10°C min^{-1} under a neutral nitrogen atmosphere at 700°C and 500°C for the ACs activated with KOH and $ZnCl_2$, respectively and maintained at activation temperature for 1 h. The carbonized samples were cooled, filtered and washed repeatedly with 0.1 M HCl followed by warm and cold deionized water until the pH of the solutions reached to neutral.

2.3. Thiol functionalized graphene oxide synthesis

Hummers method was modified for preparation of GO [17,18]. In brief, the procedure was as follows: graphite powder (10 g) was preoxidized with a solution of H_2SO_4 (200 ml), $K_2S_2O_8$ (10 g) and P_2O_5 (10 g) in an erlenmeyer flask and heated to 80°C under vigorous agitation for 24 h. Then the mixture was filtered and washed several times until rinse-water pH was reached near neutral. The filter cake was dispersed into concentrated H_2SO_4 (1 L) and $KMnO_4$ (25 g) was added slowly to the flask under strong magnetic stirring in the ice bath to prevent a sudden temperature increase. Afterward, 100 ml H_3PO_4 was added to the suspension. The dispersion was stirred continuously at 50°C for 48h and then 30% H_2O_2 (20 ml) was slowly added to the mixture resulting color change from dark brownish to brilliant yellow. Then the solution was diluted with deionized water and left overnight. Finally the suspension was filtered and washed with 10% HCl and deionized water sequentially to remove other ions.

In order to prepare TGO, GO suspension with a concentration of 1 mg/mL was obtained by dispersing GO powders (1 g) in distilled water and sonicating in an ultrasonic bath with power of 300 W for 30 min. The suspension was transferred into a round-bottom flask and 11 g Na_2SH was added and then stirred at 95°C for 6 h. Then the precipitates were filtered, washed thoroughly with deionized water, and dried in a vacuum oven at 60°C overnight to reach a constant weight [19].

2.4. Composites preparation method

To synthesis AC/TGO composites, a certain amount of ACs were soaked in 1 M nitric acid for 7 h and then filtered and washed with deionized water. Meanwhile, GO powder was added into deionized water and dispersed by ultrasonication for 60 min. AC/TGO composites were prepared by adding TGO suspension (3% wt.) into oxidized AC solutions under stirring for 15 h. Subsequently, the mixtures were placed in a water bath at 40°C, and hydrazine was carefully added into the stirred mixture until the pH of the solution became neutral. The bright yellow color of solution altered to homogeneous black indicating occurrence of the reduction. Finally, the mixture overnighted at room temperature and then filtered. The AC/TGO composites dried in a vacuum oven at 60°C for 12 h.

2.5. Characterization of ACs and AC/TGO composites

To validate successful production of AC/TGO composites and characterize the synthesized ACs and composites, Brunauer–Emmett–Teller (BET) surface area analysis (Belsorp mini II, Bel Japan Inc.), standard test for deter-

mination of iodine adsorption number (ASTM D4607-14), Fourier transform infrared (FTIR) spectroscopy (Perkin-Elmer, Model spectrum RXI), and X-ray diffraction (XRD) (Bruker D8 Advance diffractometer, Germany) with a Cu Kα anode (λ = 0.1541 nm) at 40 kV and 40 mA) and scanning electron microscopy (SEM) (Tescan, Model VEGA3)were applied. After characterization of prepared ACs and composites, the best one was selected for further experiments.

2.6. Adsorption experiments

2.6.1. Optimization of adsorption conditions

The adsorption of Pb(II) and Cu(II) onto the selected adsorbent was carried out by batch adsorption technique in an orbital shaker at a speed of 200 rpm. The samples were continually stirred at a constant temperature (25±2°C) for 60 min. At the end of this period, the adsorbents were filtered from the solutions and the concentration of metal ions were determined using a flame atomic absorption spectrophotometer (FAAS).The removal percentage of heavy metals was calculated by the following equation:

$$\text{The removal percentage } (\%) = \left(\frac{C_0 - C_e}{C_0}\right) \times 100 \quad (1)$$

where C_0 and C_e are the initial and final concentration of metal ions (mg/L), respectively. The effects of three factors namely: initial metal ions concentration, adsorbent dosage and pH were studied and optimized.

2.6.2. Kinetic and isotherm studies

The equilibrium sorption of Pb(II) and Cu(II) ions onto adsorbent were investigated in the treatment of the optimized conditions and different concentrations of Pb(II) and Cu(II) (50, 75 and 100 mg/L) agitating at ambient temperature of 25±2°C. The concentration of metal ions have no significant changes after equilibrium time. After filtration of the mixture, the filtrate was analyzed for determination the concentration of remaining Pb(II) and Cu(II) using AAS. The experimental data were fitted into Langmuir and Freundlich isotherms, the most widely used isotherm models. These isotherms relate to Pb(II) or Cu(II) adsorption per gram of synthesized adsorbent (q_e) to their equilibrium concentration (C_e). The amount of metal ions at equilibrium (q_e (mg/g)) and time t (q_t (mg/g)) were calculated as follows:

$$q_t = \left(C_0 - C_t\right)\frac{V}{W} \quad (2)$$

$$q_e = \left(C_0 - C_e\right)\frac{V}{W} \quad (3)$$

where C_0 is the initial concentration of metal ions (mg/L) and C_e and C_t are the concentrations of ions (mg/L) at equilibrium and time t, respectively. V is the volume of the solution (L) and W is the weight (g) of used adsorbent. The controlling mechanisms of Pb(II) and Cu(II) adsorption process onto the adsorbent such as mass transport process and chemical reaction were investigated using two kinetic models: pseudo first order and pseudo second order.

2.6.3. Determination of the effect of competing ions

To determine the effects of possible interference of secondary cations on the adsorption of Pb(II) and Cu(II) by AC/TGO, the solutions containing 5, 10, 50, 100 and 200 mg/L of Na(I), Mg(II) and Ca(II) were spiked with 50 mg/L of either Cu(II) or Pb(II) and 0.5 g/L of AC/TGO and shaken 1 h, at a speed of 200 rpm. Then they were filtered and the residual concentrations of heavy metals in the filtrate were analyzed as stated above.

2.6.4. Regeneration studies

The adsorption process was conducted under optimized conditions and the optimum amount of KAC/TGO loaded with either Pb(II) or Cu(II) was obtained. The adsorbent was dried in an oven at 35°C for 24 h and added into 100 ml of 0.1 M solution of HNO_3, HCl and $NaNO_3$ as the eluting agents. The samples were shaken (200 rpm at 25±2°C) for 1 h and the effluent was analyzed to determine the concentration of Cu(II) or Pb(II) desorbed by the KAC/TGO. The adsorption desorption procedure of KAC/TGO with the best desorbing agent were repeated 3 times on the same matrix to establish the reusability of KAC/TGO. The percentage of desorbed metal was calculated by the following equations:

$$\text{Desoption } (\%) = \left[\frac{q_{des}}{q_{ads}}\right]100 \quad (4)$$

$$q_{des} = C_{des}\frac{V}{W} \quad (5)$$

where q_{des} is the content of desorbed metal (mg/g), C_{des} (mg/L) is concentration of metal ion in the solution with volume V (L), and W is adsorbent weight (g).

3. Results and discussion

3.1. Characteristics of prepared composites

FTIR was used to determine surface functional groups of TGO, ACs and AC/TGO composites (Fig. 1a). The absorption bands ascribe mainly to hydroxyl and carbonyl groups on the surface of adsorbents. Broadened peak around 3400 cm^{-1} is identical to the bands of the bonded –OH groups due to vibration of water molecules revealing that the TGO in the composites contain a large amount of adsorbed water. The peaks at 2900 cm^{-1} are associated with the aliphatic C–H symmetric groups. The bands observed at 1422 cm^{-1} can be usually assigned to the oxygen containing functional groups stretching vibration, such as C=O and C–O of carboxylic groups [20] or the O–H in-plane vibration of carboxylic group [21]. Another peaks at 2400 cm^{-1} rise due to the presence of –C≡C groups[22]. The week bands in the range of 900–1300 cm^{-1} may be due to the presence of C–O groups in the samples [20]. The intense band found at 874 cm^{-1} assigns to the stretching vibrations of C-H out-of-plane bend.

Degrees of order and structure of TGO, ACs and AC/TGO composites were examined using XRD over the 2θ range 3–80° with a step size of 0.05° per step (Fig. 1b). Pres-

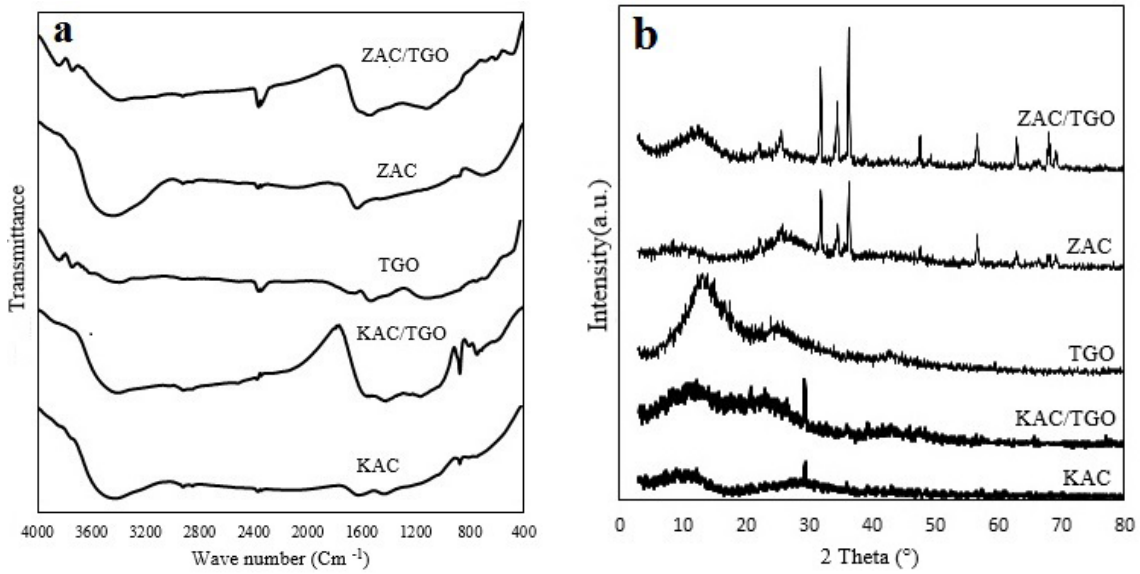

Fig. 1. FTIR (a) and XRD (b) spectra of composites, ACs and TGO.

ence of micropores and microcrystallinity cause enhanced background signal between 10–20° due to scattering the X-ray beam as a result of graphite-like microcrystalline structure of multilayer stacks [23]. A broad peak around 2θ = 11 corresponds to the diffraction peak of TGO. The XRD patterns show two diffraction peaks at 2θ = 25° and 45–47.5 corresponding to the formation of hexagonal graphite structures and turbostratic structure of disordered carbon. Also the noticeable humps in the range between 20 to 30° are identical of carbonaceous substances [20]. The peak at 2θ = 21° provides evidence for the presence of the stacking structure of graphite [21].The results of XRD patterns of KAC and KAC/TGO show that they may contain potassium compounds with high crystallinity as a result of activation the activated carbon with KOH. Also K_2CO_3, K_2O and metallic K are the dominant potassium compounds that are produced in the reaction between KOH and surface carbon [24]. Small peaks at 30.2°, 31.5° related to the peaks corresponding to K_2CO_3. The diffraction peak around 2θ = 23° relate to the ordered K/graphite. XRD spectra of the ZAC and ZAC/TGO also shows sharp narrow peaks at 2θ = 32°, 34.65°, 47° and 56.75° providing evidence for the presence of zinc oxide and zinc carbids. Also, the sharp diffraction peaks at 2θ = 36.45° are related to the metallic Zn [25]. Other peaks where located around 2θ = 69° show some impurities.

N_2 adsorption/desorption measurements at 77 K was used for determination of textural properties of ACs and AC/TGO composites (Table 1 and Fig. 2). The sharp knees of the curves indicate an increased adsorption of N_2 at low relative pressure (below 0.1) and micropore filling effect. The increase in N_2 adsorbed volume at higher pressure (in the range of 0.1–1) is associated with the multilayer adsorption and capillary condensation in mesoporous materials which is usually accompanied by the presence of hysteresis loops. The N_2 adsorption desorption isotherms of ACs and AC/TGO composites seem to be a combination of types I and IV, reflecting the presence of both micro and mesopores in their structures.

SEM studies were performed to investigate the topographic features of ACs and composites. As shown in Fig. 3, ZAC surface is a kind of honeycomb structure and KAC surface has sponge like pores with different sizes and shapes. SEM micrographs show well-developed porosity and indicate the external surface of ACs and composites have wide cracks, crevices and cavities. Few crystals in the pores are most probably potassium and zinc compounds as a result of AC activation with KOH and $ZnCl_2$. TGO sheets are distributed over carbon particles and in the holes. By comparing the results obtained from the characterization of the ACs and composites, KAC/TGO was selected for all further experiments.

3.2. Adsorption studies

3.2.1. Effect of initial metal ions concentration, adsorbent dosage and pH

To find the optimum initial concentration of Pb(II) and Cu(II) for the effective adsorption onto the KAC/TGO, the experiments were conducted at different initial metal ions concentrations from 30–120 mg/L containing 0.05 g adsorbent in 100 ml either Pb(II) or Cu(II) solutions at pH 6. As illustrated in Fig. 4a, the adsorption efficiency of KAC/TGO increase initially and then decrease from 84.58% to 62.98% for Pb solution at concentration of 50 mg/L and 120 mg/L respectively. Also removal percentage of Cu(II) increase to 78.67% at concentration of 60 mg/L and then decrease to 48.54% at concentration of 120 mg/L. The percentage removal decreased with increasing the initial concentration of metal ions above 50 mg/L and 60 mg/L for Pb and Cu solutions, respectively, because of an increase in the driving force of the concentration gradient.

The influence of KAC/TGO dosage (0.02–0.08 g/100 mL) on the adsorption of Pb(II) and Cu(II) ions was investigated by employing optimum Pb(II) and Cu(II) concentration at pH 6 for 60 min. According to the results (Fig. 4b), Pb(II) and Cu(II) removal percentage increased from 48.66% to 86.8% and 40.63% to 83.8%, respectively when the KAC/TGO dos-

Table 1
Textural properties of the prepared ACs and composites

	S_{BET} (m^2/g)	t-plot micropore surface area (m^2/g)	t-plot external surface area (m^2/g)	Total pore Volume (m^3/g)	t-plot micropore volume (m^3/g)	Pore size (nm)	Iodine number (mg/g)
KAC	757	476	281	0.759	0.223	4	674
ZAC	621	349	272	0.694	0.162	4.4	585
KAC/TGO	1044	651	393	0.998	0.306	3.82	920
ZAC/TGO	846	513	332	0.778	0.246	3.67	760

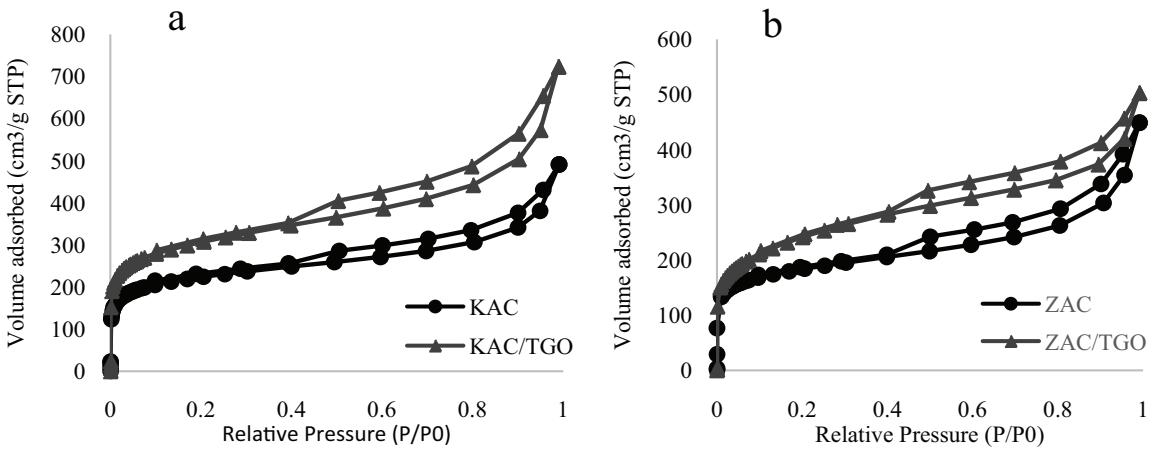

Fig. 2. N_2 adsorption/desorption isotherms of the prepared ACs and composites using KOH (a) and $ZnCl_2$ (b) activation.

age increased from 0.02–0.05 g/100 mL. But no significant change in metal ions removal percentage was observed with further dosage increase to 0.07 g/100 mL (89.46% and 87.06% for Pb(II)and Cu(II), respectively). It can be understood that increasing the number of available adsorption sites as well as total surface area are related to increasing KAC/TGO dosage. It is apparent that the percentage of heavy metals adsorbed per unit mass of KAC/TGO reduced by increasing adsorbent dose. Remaining unsaturated of adsorption sites during the adsorption process can cause decreasing adsorption density with dose increment. These observations are in accordance with other reported studies on the adsorption of metals ions by different adsorbents [26,27].

pH is an important factor for increasing the removal efficiency of Pb(II) and Cu(II) ions through adsorption process onto KAC/TGO, because the solubility and mobility of metal ions, chemical characteristic of the aqueous solution, degree of ionization and speciation of the adsorbate and also concentration of the counter ions on the surface functional groups of KAC/TGO are affected by pH. Batch adsorption was carried out in aqueous solutions (100 mL) containing the optimum amount of KAC/TGO for 60 min. The initial pH of the solution was adjusted to the desired values (in the range of 3–7) by adding 0.1 M HCl or 0.1 M NaOH. The metal ions adsorption onto KAC/TGO increased when the initial pH of the solutions were increased from 3–5 and then decreased at pH > 5 (Fig. 4c). Similar results were reported by Sitko et al. [28], Rahimi et al. [29] and Shi et al. [30].

Initial pH affects the adsorption process by changing the surface charge of the adsorbent. The lowest Pb(II) and Cu(II) adsorption rates were obtained at pH = 3. At lower pH, the active sites such as hydroxyl groups on the surface of KAC/TGO are closely associated with the hydronium ions. Therefore, the adsorption of Pb(II) and Cu(II) ions is partially inhibited on the sorption site, possibly due to the competition between H^+ ions and cationic ions for the active surface sites. At pH lower than 5.0, the approach of Pb(II) and Cu(II) to the composite surface is restricted as a result of repulsive forces and this prevents the adsorption of these metal ions onto KAC/TGO [31]. At moderate pH, deprotonation of KAC/TGO is occurs and its surface becomes more negatively charged and electrostatically attracts metal ions with positive charge. This in turn contributes to increase the adsorbate removal from the solution. At the same time, hydroxyl groups dissociated from the surface of KAC/TGO react with metal ions and form species with low solubility such as $PbOH^+$, $Pb(OH)_4^{2-}$, $Pb(OH)_2$ and $Cu(OH)_2$, which leads to an increase in the removal percentage [32,33]. The pH above 6 was not considered in the current research, because Pb(II) and Cu(II) precipitation occur in the medium.

3.2.2. Adsorption isotherms

A Freundlich isotherm model is an empirical equation assumes that the adsorbent involves heterogeneous sorption base with several adsorption energies. The logarithmic form of the Freundlich equation is given by [34]:

$$\log(q_e) = \log k_f + 1/\mathrm{n} \log C_e \quad (6)$$

where K_f and $1/n$ are considered as Freundlich model constants that they are related to the measured adsorption

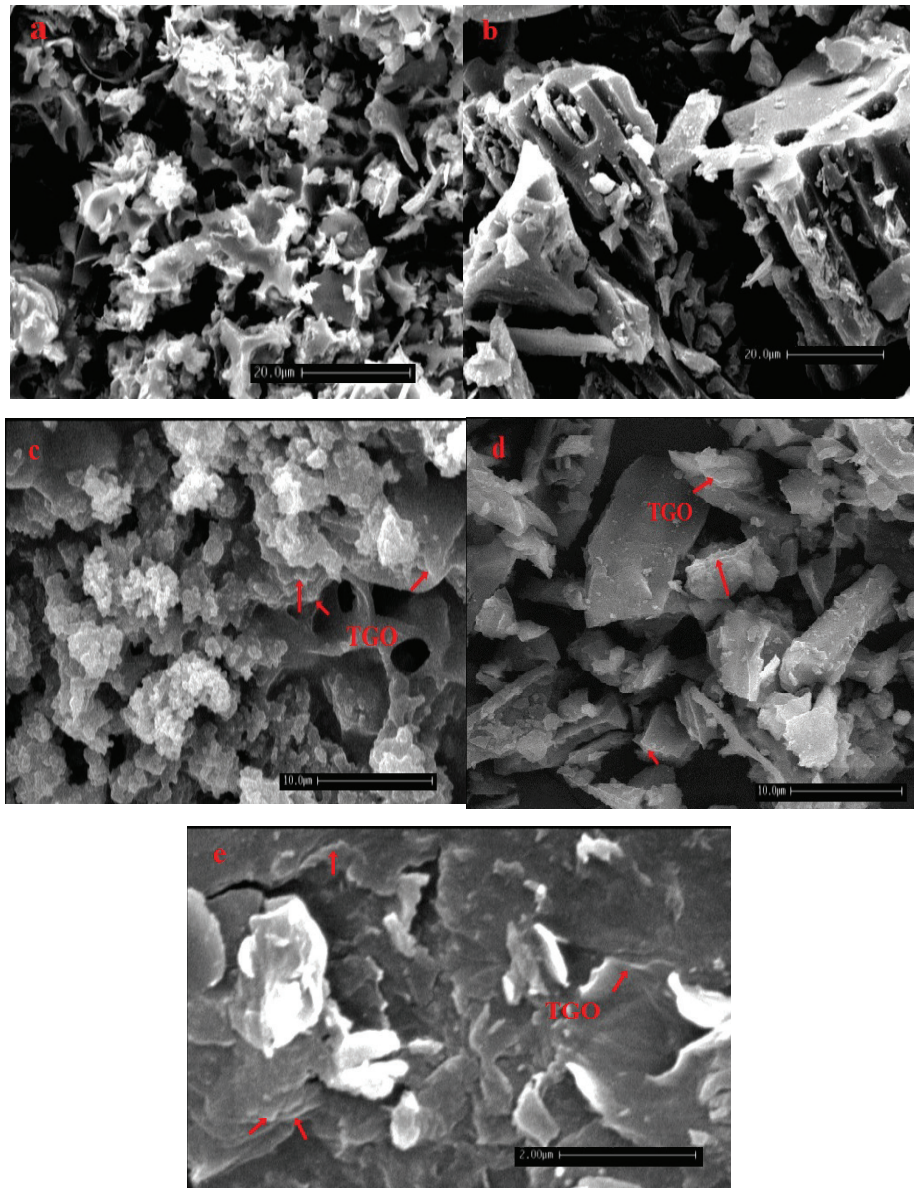

Fig. 3. SEM images of ZAC (a), KAC (b) ZAC/TGO (c), KAC/TGO (d) and TGO (e).

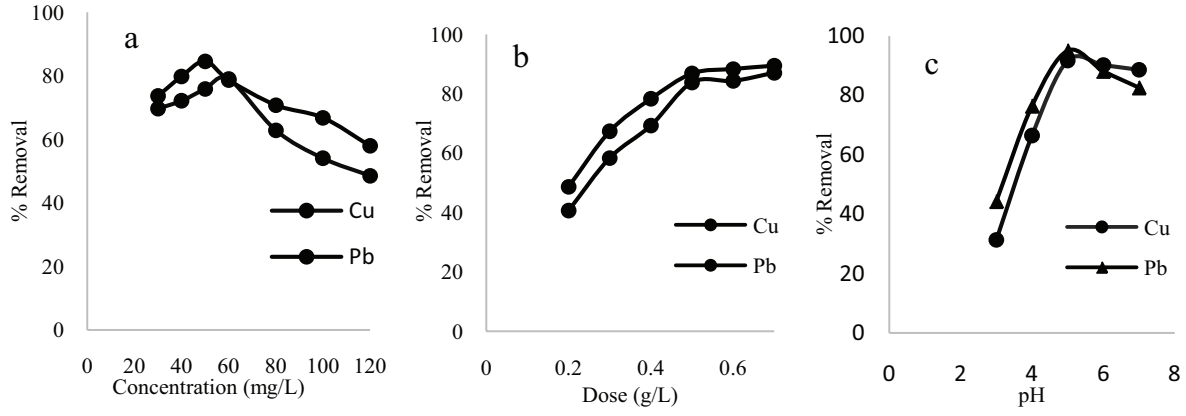

Fig. 4. Effect of initial concentration (a), KAC/TGO dose (b) and pH (c) on the removal of Pb(II) and Cu(II) ions.

capacity of adsorbent and adsorption intensity, respectively. To examine the ability of the Freundlich model to fit the experimental equilibrium data, log C_e was plotted versus log q_e and K_f and n were determined from the intercept and the slop of produced straight line fitted to the data (Fig. 5a). The magnitudes of K_f and n present desirable uptake and easy separation of adsorbate from the aqueous solution.

Langmuir isotherm assumes a monolayer adsorbent with a homogeneous surface containing similar sorption sites that adsorption energies are uniform on its surface. Thus, Langmuir isotherm describes the equilibrium behavior of solute between the adsorbent and the solution. The linearized form of Langmuir equation is as follows [35]:

$$\frac{C_e}{q_e}=\frac{1}{q_m}C_e+\frac{1}{K_L q_m} \tag{7}$$

where q_m and K_L are the Langmuir isotherm constants related to the maximum monolayer coverage capacity (mg/g) and the energy of adsorption (L/mg), respectively. C_e is the equilibrium concentration of metal ion (mg/L) and q_e is the amount of metal ion uptake per gram of KAC/TGO at equilibrium (mg/g). The values of q_m and K_L can be calculated from the slope and intercept of the line obtained by plotting vs. C_e. The essential characteristic of a Langmuir equation can be evaluated by means of "R_L", a dimensionless steady called separation factor or equilibrium parameter which can be calculated by using the equation below:

$$R_L=\frac{1}{1+\left(1+K_L C_e\right)} \tag{8}$$

The value of R_L assumes the adsorption feasibility and nature to be either unfavorable ($R_L > 1$), linear ($R_L = 1$), favorable ($0 < R_L < 1$) and irreversible ($R_L = 0$). All values of R_L at different initial concentrations of Pb(II) Cu(II) were in the range of 0–1 demonstrating highly favorable adsorption of these metal ions onto the KAC/TGO.

The Langmuir and Freundlich constants with the correlation coefficients are shown in Table 2. According to the high values of correlation coefficient, the Langmuir model describes the adsorption process better than Freundlich model. Based on comparison of maximum monolayer adsorption capacity (q_m of Pb(II) and Cu(II) onto different reported adsorbent (Table 3), it can be concluded that KAC/TGO is a promising adsorbent with a very large adsorption capacity to uptake Pb(II) and Cu(II) from wastewater.

3.2.3. Adsorption kinetics

To determine the adsorption kinetics of Pb(II) and Cu(II) onto the KAC/TGO, the pseudo-first order and pseudo-second order kinetic models were used. The pseudo first order equation is represented as follows [44]:

$$\log\left(q_e-q_t\right)=\log q_e-\frac{K_{ad}}{2.303}\cdot t \tag{9}$$

where q_t is adsorbed amount of solute at certain time t (mg/g) and K_{ad} (min^{-1}) is the pseudo-first order rate constant (min^{-1}). The values of the rate constant and the correlation coefficient at different initial concentrations of Pb(II)and Cu(II) ions were determined by plotting a graph between log ($q_e - q_t$) vs. t (Fig. 6(a) and (c) and Table 4).

The pseudo-second-order kinetic model is expressed as:

$$\frac{t}{q_t}=\frac{1}{h}+\frac{1}{q_e}t \tag{10}$$

where the initial adsorption rate, h (mg/g·min) is equal to $K_2 q_e^2$ and K_2 is the rate constant of the pseudo second order adsorption (g/mg·min) and can be obtained from the slope ($1/q_e$) and intercept ($1/h$) of the linear plot of (t/q_t) vs. t. The plots of the linearized form of the pseudo- second order kinetic model (t/q_t vs. t) at different initial concentrations of Pb(II) and Cu(II) are shown in Fig. 6(b) and (d). The values

Table 2
The Langmuir and Freundlich models constants and correlation coefficients

Heavy metal	Langmuir isotherm			Freundlich isotherm		
	q_m (mg/g)	K_L (L/mg)	R^2	K_f (mg/g) (L/mg)$^{1/n}$	n	R^2
Pb(II)	204.08	0.42	0.9999	77.66	3.28	0.9822
Cu(II)	196.07	0.29	0.9953	65.65	3.02	0.8899

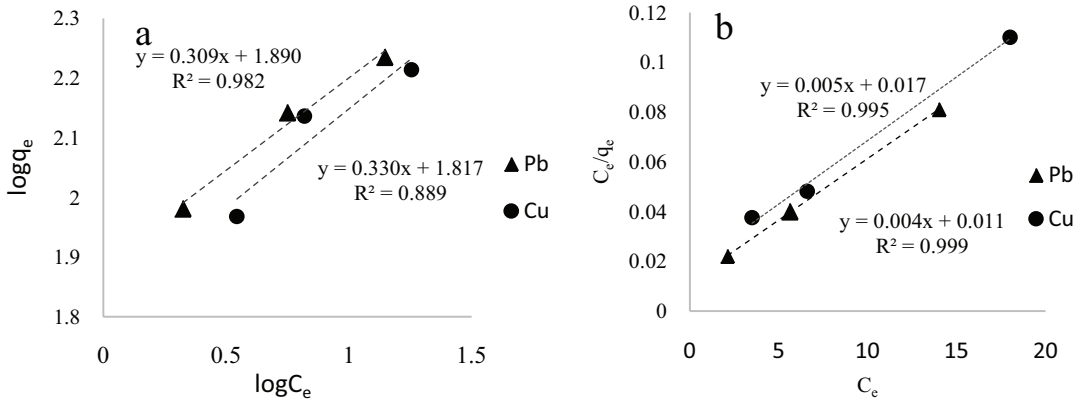

Fig. 5. Linear plots for the Freundlich (a) and Langmuir (b) isotherm models.

Table 3
Maximum monolayer adsorption of Pb(II) and Cu(II) onto different reported adsorbents

Heavy metal	Adsorbents	(mg/g)	Ref.
Pb(II)	bentonite clay based hydroxyapatite composite	346	[36]
Pb(II)	AC/G	217/6	[13]
Pb(II), Cu(II)	EDTA-functionalized chitosan/GO	206.52, 207.26	[37]
Pb(II), Cu(II)	KAC/TGO	204.08, 196.07	This study
Pb(II)	AC (from citrus limettioidesseed)	142.86	[38]
Pb(II), Cu(II)	carbon nanotube/graphene hybrid aerogels	104.9, 33.8	[39]
Pb(II)	baelleaves (aeglemarmelos)	104.00	[40]
Pb(II)	chemically treated rubber leaf powder	95.30	[41]
Cu(II)	magnetic copper imprinted chitosan/GO composite	132	[42]
Cu(II)	amidoximated polyacrylonitrile/organobentonite composite	77.43	[43]

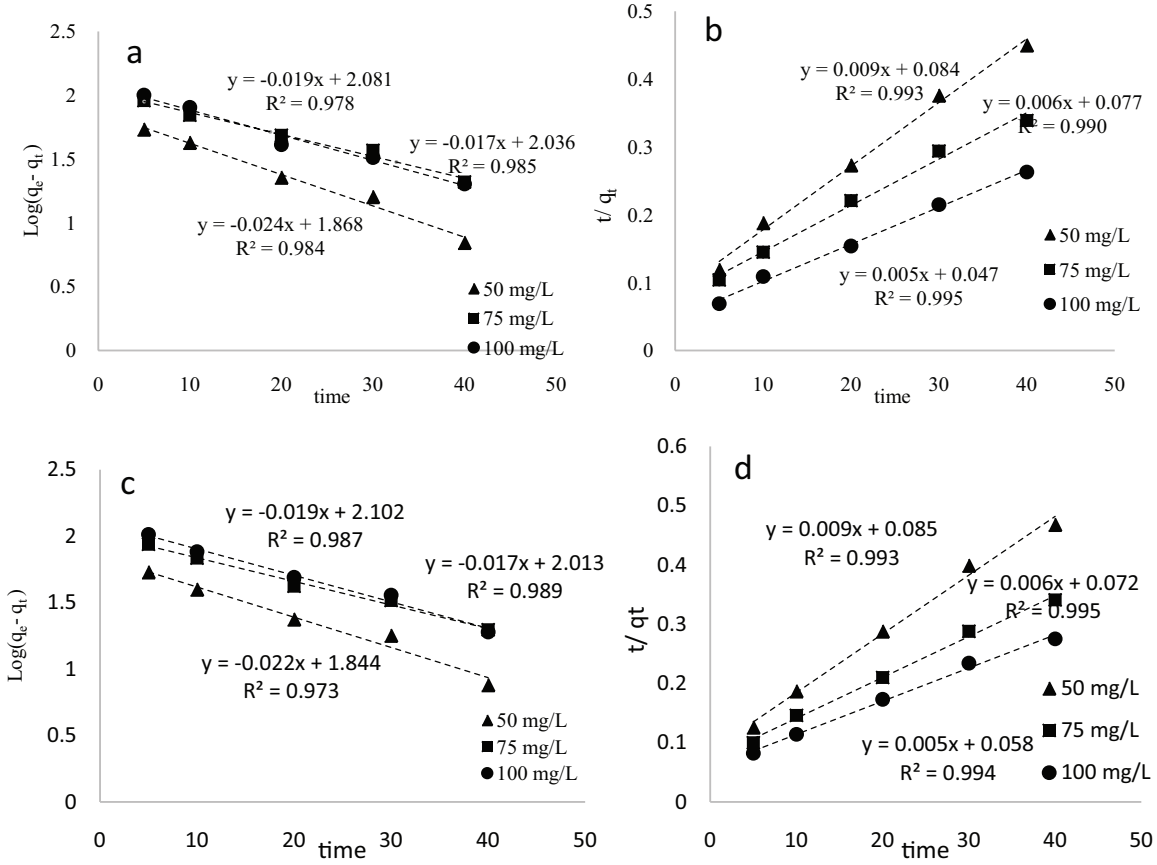

Fig. 6. Linear plots for the pseudo-first order (a) and pseudo-second order (b) kinetics of Pb(II) and linear plots for the pseudo-first order (c) and pseudo-second order (d) kinetics of Cu(II).

of constant parameters and correlation coefficients calculated for pseudo-second order kinetic model are presented in Table 4. Highest correlation coefficients (R^2) were belong to the pseudo-second order, indicating the studied adsorption system are in the good agreement with pseudo-second order kinetic model. These results validate this assumption that the rate limiting step of Pb(II) and Cu(II) uptake on the KAC/TGO is presumably chemisorption. This kind of adsorption typically involves chemical reaction between the adsorbate and the KAC/TGO surface by generating new chemical (usually covalent) bonds and metal ions prefer to occupy the sites that maximize their coordination number with the substrate.

3.2.4. Effect of competing ions

Natural waters and industrial effluents contain common metal ions such as sodium, calcium and magnesium

Table 4
Pseudo-first order and pseudo-second order adsorption rate constants, q_e and R^2 values

	Metal ion concentration (mg/L)	Pseudo-first-order rate equation			Pseudo-second-order rate equation			
		K_{ad} (min^{-1})	q_e (mg/g)	R^2	K_2 (g/mg-min)	q_e (mg/g)	h (mg/g-min)	R^2
Pb(II)	50 mg/L	0.056	73.87	0.9849	0.1×10^{-2}	106.38	11.86	0.9939
	75 mg/L	0.039	108.76	0.9854	6×10^{-4}	147.05	12.99	0.9902
	100 mg/L	0.045	120.67	0.9789	6.3×10^{-4}	181.81	21.1	0.9955
Cu(II)	50 mg/L	0.052	69.83	0.9733	1.1×10^{-2}	101.01	11.68	0.9931
	75 mg/L	0.040	103.20	0.9898	6.5×10^{-4}	144.92	13.85	0.995
	100 mg/L	0.045	126.50	0.9876	5.4×10^{-4}	178.58	17.24	0.9947

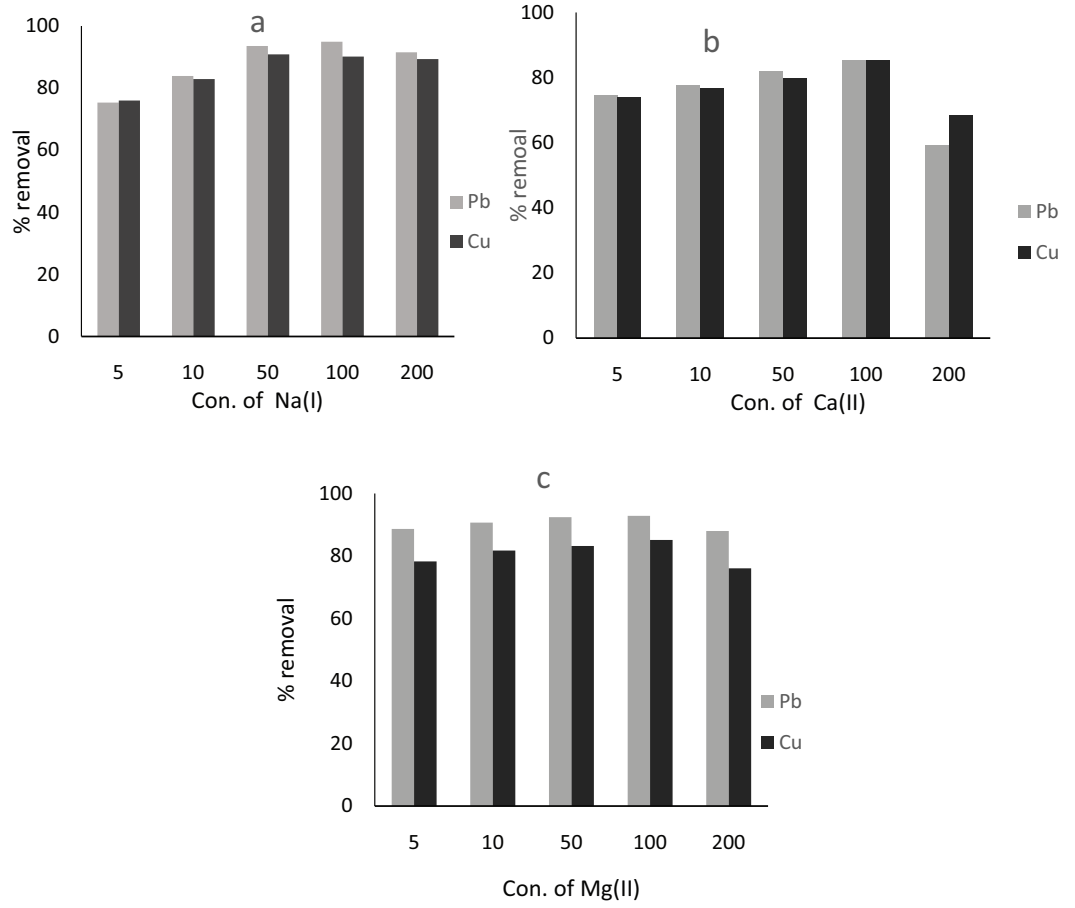

Fig. 7. Effect of increasing concentrations of Na(I) ions (a), Ca(II) ions (b) and Mg(II) ions (c) on the adsorption of Pb(II) and Cu(II) by KAC/TGO.

cations, in significant concentrations. These cations compete for binding sites of the adsorbents and affect their metal sorption potential [45]. Therefore, it is necessary to determine the competition between the heavy metals and various concentrations of these cations for adsorption onto AC/TGO. Fig. 10 shows the effects of competition of naturally occurring interfering cations Na(I), Mg(II) and Ca(II) on the adsorption of the selected heavy metals by the AC/TGO. Na(I) as a monovalent cation showed the lowest effect on the binding of target metal ions onto the adsorbent, because it does not directly compete with divalent cations for binding sites of AC/TGO. However, in the presence of Na(I) at 5 mg/L, Pb(II) and Cu(II) uptake were reduced approximately 22 and 15%, respectively. At 200 mg/L of Ca(II) ions, the adsorptions of Cu(II) and Pb(II) were approximately reduced by 23% and 36% , respectively. This adsorption can also be due to the increase in ionic strength of the solution because of the higher number of charged species.

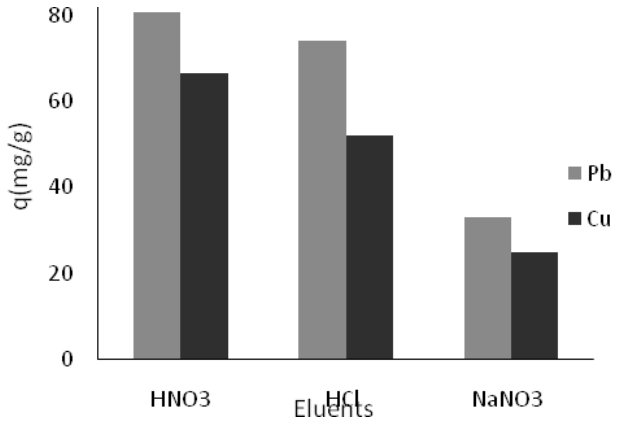

Fig. 8. Comparison of different desorbing agents on the desorption of Pb(II) and Cu(II).

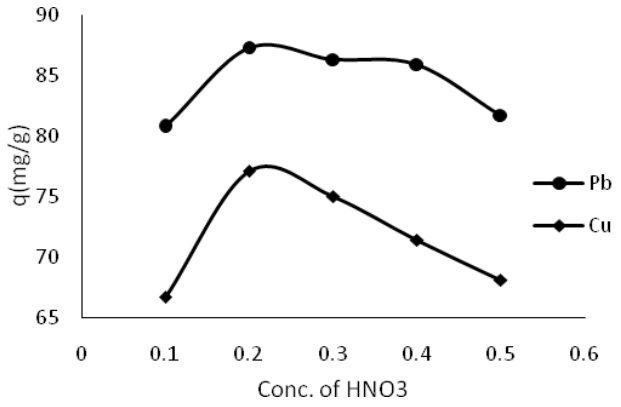

Fig. 9. Effect of different concentrations of HNO_3 on the desorption of Pb(II) and Cu(II).

3.2.5. Regeneration studies

Adsorption desorption experiments were conducted through batch studies to examine the reversibility of the adsorption process and the feasibility of adsorption and desorption behavior of KAC/TGO for Pb(II) and Cu(II) removal. The concentration of metal ions in each solution is shown in Fig. 8. The most effective desorbing agent for desorption of both metals and regenerating the adsorbent was found to be 0.1 M HNO_3. Under acidic condition, the KAC/TGO was protonated by H^+ ions to promote desorption of positively charged metal ions from its surface. Desorption experiments were performed at different concentrations of HNO_3 (0.1–0.5 M), to investigate the effects of different concentrations of the eluting agent. According to the results, maximum desorption was achieved by 0.2 M HNO_3 (Fig. 9). In order to investigate the adsorbent regeneration ability, consecutive adsorption–desorption cycles were repeated three times using recycled KAC/TGO as the regenerated sorbent and 0.2 M HNO_3 as the effective eluting agent (Fig. 10).

4. Conclusion

High surface area KAC/TGO composite was synthesized successfully from thiol functionalized graphene oxide and AC prepared from sugar cane molasses using KOH activation. The experiments were focused on the use of this composite for removal of lead and copper ions from aqueous solutions. The maximum adsorption capacities of KAC/TGO were found to be 204.08 and 196.07 mg/g for Pb(II) and Cu(II), respectively. Optimum conditions obtained at pH 5.0, the adsorbent mass of 0.05 g/100 mL and initial metal ion concentration of 50 mg/L and 60 mg/L for Pb(II) and Cu(II), respectively. The adsorption process was found to conform to the pseudo-second-order kinetic model and the equilibrium data of the study followed the Langmuir adsorption isotherm. Hence, heavy metals adsorption on the KAC/TGO is mostly homogeneous and monolayer adsorption. The most effective agent for desorbing Pb(II) and Cu(II) ions from KAC/TGO was observed to be 0.2 M HNO_3. Regenerating of KAC/TGO demonstrates that it can be infinitely reused in acid treatment for adsorbing Pb(II) and Cu(II) repeatedly from aqueous solutions without significant loss in its adsorption capacity. Fast and facile production, nanometer size, low cost and high adsorption capacity make KAC/TGO as a new promising adsorbent in water and wastewater treatment for removal of heavy metals.

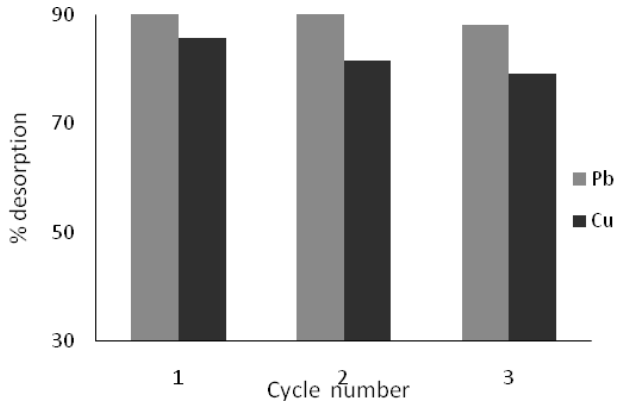

Fig. 10. Three sequential adsorption–desorption cycles of AC/TGO for Pb(II) and Cu(II) removal using 0.2 M HNO_3.

References

[1] M. Karnib, A. Kabbani, H. Holail, Z. Olama, Heavy metals removal using activated carbon, silica and silica activated carbon composite, Enrgy. Proced., 50 (2014) 113–120.
[2] M. Barakat, New trends in removing heavy metals from industrial wastewater, Arab. J. Chem., 4 (2011) 361–377.
[3] J. Shou, M. Qiu, Adsorption of copper ions onto activated carbon from capsicum straw, Desal. Water Treat., 57 (2016) 353–359.
[4] S. Veli, B. Alyüz, Adsorption of copper and zinc from aqueous solutions by using natural clay, J. Hazard. Mater., 149 (2007) 226–233.
[5] O.E.A. Salam, N.A. Reiad, M.M. ElShafei, A study of the removal characteristics of heavy metals from wastewater by low-cost adsorbents, J. Adv. Res., 2 (2011) 297–303.
[6] M.M. Shahata, Adsorption of some heavy metal ions by used different immobilized substances on silica gel, Arab. J. Chem., 9 (2016) 755–763.
[7] G. Crini, Non-conventional low-cost adsorbents for dye removal: a review, Biores. Technol., 97 (2006) 1061–1085.

[8] M. Yari, M. Norouzi, A.H. Mahvi, M. Rajabi, A. Yari, O. Moradi, I. Tyagi, V.K. Gupta, Removal of Pb (II) ion from aqueous solution by graphene oxide and functionalized graphene oxide-thiol: effect of cysteamine concentration on the bonding constant, Desal. Water Treat., 57 (2016) 11195–11210.
[9] S. Peng, H. Meng, Y. Ouyang, J. Chang, Nanoporous magnetic cellulose–chitosan composite microspheres: preparation, characterization, and application for Cu (II) adsorption, Ind. Eng. Chem. Res., 53 (2014) 2106–2113.
[10] L. Li, C. Luo, X. Li, H. Duan, X. Wang, Preparation of magnetic ionic liquid/chitosan/graphene oxide composite and application for water treatment, Int. J. Biol. Macromol., 66 (2014) 172–178.
[11] I. Sheet, A. Kabbani, H. Holail, Removal of heavy metals using nanostructured graphite oxide, silica nanoparticles and silica/graphite oxide composite, Enrgy. Proced., 50 (2014) 130–138.
[12] L. Xu, J. Li, M. Zhang, Adsorption characteristics of a novel carbon-nanotube-based composite adsorbent toward organic pollutants, Ind. Eng. Chem. Res., 54 (2015) 2379–2384.
[13] N. Saeidi, M. Parvini, Z. Niavarani, High surface area and mesoporous graphene/activated carbon composite for adsorption of Pb (II) from wastewater, JECE., 3 (2015) 2697–2706.
[14] A.A. Rahim, Z.N. Garba, Optimization of preparation conditions for activated carbon from Prosopis africana seed hulls using response surface methodology, Desal. Water Treat., 57 (2016) 17985–17994.
[15] L. Wang, M. Zhang, Z. Huang, C. Zhao, X. Pei, Adsorption mechanism of activated carbon fibre/carbon nanotube composites for rhodamine b from aqueous solution, Asian J. Chem., 25 (2013) 10509.
[16] E.P. Randviir, D.A. Brownson, C.E. Banks, A decade of graphene research: production, applications and outlook, Mater. Today., 17 (2014) 426–432.
[17] W.S. Hummers Jr, R.E. Offeman, Preparation of graphitic oxide, J. Am. Chem. Soc., 80 (1958) 1339–1339.
[18] X. Li, S. Wang, Y. Liu, L. Jiang, B. Song, M. Li, G. Zeng, X. Tan, X. Cai, Y. Ding, Adsorption of Cu (II), Pb (II), and Cd (II) ions from acidic aqueous solutions by diethylenetriaminepentaacetic acid-modified magnetic graphene oxide, J. Chem. Eng. Data., 62 (2016) 407–416.
[19] M. Yun, M.S. Ahmed, S. Jeon, Thiolated graphene oxide-supported palladium cobalt alloyed nanoparticles as high performance electrocatalyst for oxygen reduction reaction, J. Power. Sources., 293 (2015) 380–387.
[20] E. Köseoğlu, C. Akmil-Başar, Preparation, structural evaluation and adsorptive properties of activated carbon from agricultural waste biomass, Adv. Powder Technol., 26 (2015) 811–818.
[21] Y. Gao, Q. Yue, B. Gao, Y. Sun, W. Wang, Q. Li, Y. Wang, Comparisons of porous, surface chemistry and adsorption properties of carbon derived from Enteromorpha prolifera activated by $H_4P_2O_7$ and KOH, Chem. Eng. J., 232 (2013) 582–590.
[22] N.K. Mondal, R. Bhaumik, J.K. Datta, Removal of fluoride by aluminum impregnated coconut fiber from synthetic fluoride solution and natural water, AEJ., 54 (2015) 1273–1284.
[23] Y. Huang, E. Ma, G. Zhao, Thermal and structure analysis on reaction mechanisms during the preparation of activated carbon fibers by KOH activation from liquefied wood-based fibers, Ind. Crop. Prod., 69 (2015) 447–455.
[24] Y. Ji, T. Li, L. Zhu, X. Wang, Q. Lin, Preparation of activated carbons by microwave heating KOH activation, Appl. Surf. Sci., 254 (2007) 506–512.
[25] H. Sayğılı, F. Güzel, High surface area mesoporous activated carbon from tomato processing solid waste by zinc chloride activation: process optimization, characterization and dyes adsorption, J. Clean Prod., 113 (2016) 995–1004.
[26] Z. Melichová, L. Hromada, Adsorption of Pb^{2+} and Cu^{2+} ions from aqueous solutions on natural bentonite, Pol. J. Environ. Stud., 22 (2013) 457–464.
[27] Z. Liu, S. Zhou, Adsorption of copper and nickel on Na-bentonite, Process Saf. Environ., 88 (2010) 62–66.
[28] R. Sitko, E. Turek, B. Zawisza, E. Malicka, E. Talik, J. Heimann, A. Gagor, B. Feist, R. Wrzalik, Adsorption of divalent metal ions from aqueous solutions using graphene oxide, Dalton T., 42 (2013) 5682–5689.
[29] S. Rahimi, R.M. Moattari, L. Rajabi, A.A. Derakhshan, M. Keyhani, Iron oxide/hydroxide (α, γ-FeOOH) nanoparticles as high potential adsorbents for lead removal from polluted aquatic media, J. Ind. Eng. Chem., 23 (2015) 33–43.
[30] B. Shi, W. Zuo, J. Zhang, H. Tong, J. Zhao, Removal of lead(II) ions from aqueous solution using L. seed husk ash as a biosorbent, J. Environ. Qual., 45 (2016) 984–992.
[31] A. Bhatnagar, E. Kumar, M. Sillanpää, Fluoride removal from water by adsorption—a review, Chem. Eng. J., 171 (2011) 811–840.
[32] C.K. Ko, W.G. Lee, Effects of pH variation in aqueous solutions on dissolution of copper oxide, Surf. Interface Anal., 42 (2010) 1128–1130.
[33] E. Sočo, J. Kalembkiewicz, Comparison of adsorption of Cd(II) and Pb(II) ions on pure and chemically modified fly ashes, Chem. Process. Eng., 37 (2016) 215–234
[34] H. Freundlich, Über die adsorption in lösungen, Z. Phys. Chem., 57 (1907) 385–470.
[35] I. Langmuir, The adsorption of gases on plane surfaces of glass, mica and platinum, J. Am. Chem. Soc., 40 (1918) 1361–1403.
[36] P.R. Choudhury, P. Mondal, S. Majumdar, Synthesis of bentonite clay based hydroxyapatite nanocomposites cross-linked by glutaraldehyde and optimization by response surface methodology for lead removal from aqueous solution, RSC Adv., 5 (2015) 100838–100848.
[37] A. Shahzad, W. Miran, K. Rasool, M. Nawaz, J. Jang, S.-R. Lim, D.S. Lee, Heavy metals removal by EDTA-functionalized chitosan graphene oxide nanocomposites, RSC Adv., 7 (2017) 9764–9771.
[38] R. Sudha, K. Srinivasan, P. Premkumar, Batch studies for the adsorption of lead (II) from aqueous phase by waste generated from Citrus Limettioides, Int. J. Chem. Sci., 13 (2015) 167–177.
[39] Z. Sui, Q. Meng, X. Zhang, R. Ma, B. Cao, Green synthesis of carbon nanotube–graphene hybrid aerogels and their use as versatile agents for water purification, J. Mater. Chem., 22 (2012) 8767–8771.
[40] S. Chakravarty, A. Mohanty, T.N. Sudha, A. Upadhyay, J. Konar, J. Sircar, A. Madhukar, K. Gupta, Removal of Pb(II) ions from aqueous solution by adsorption using bael leaves (Aegle marmelos), J. Hazard. Mater., 173 (2010) 502–509.
[41] M.H.M.A. Kamal, W.M.K.W.K. Azira, M. Kasmawati, Z. Haslizaidi, W.N.W. Saime, Sequestration of toxic Pb(II) ions by chemically treated rubber (Hevea brasiliensis) leaf powder, J. Environ. Sci., 22 (2010) 248–256.
[42] D. Kong, N. Wang, N. Qiao, Q. Wang, Z. Wang, Z. Zhou, Z. Ren, Facile preparation of ion-imprinted chitosan microspheres enwrapping Fe_3O_4 and graphene oxide by inverse suspension cross-linking for highly selective removal of Copper(II), ACS Sustain. Chem. Eng., 5 (2017) 7401–7409.
[43] T. Anirudhan, M. Ramachandran, Synthesis and characterization of amidoximated polyacrylonitrile/organobentonite composite for Cu(II), Zn(II), and Cd(II) adsorption from aqueous solutions and industry wastewaters, Ind. Eng. Chem. Res., 47 (2008) 6175–6184.
[44] S. Lagergren, About the theory of so-called adsorption of soluble substances. K. Sven. vetensk.akad. handl., 24 (1898) 1–39.
[45] X. Gao, Y. Hu, T. Guo, X. Ye, Q. Li, M. Guo, H. Liu, Z. Wu. Comparative study of the competitive adsorption of Mg, Ca and Sr ions onto resins, Adsorpt. Sci. Technol., 31 (2013) 45–58.